



Pergamon

Neuropharmacology 43 (2002) 11–27

NEURO
PHARMACOLOGY

www.elsevier.com/locate/neuropharm

Selective enhancement of AMPA receptor-mediated function in hippocampal CA1 neurons from chronic benzodiazepine-treated rats

Bradley J. Van Sickle, Elizabeth I. Tietz *

Department of Pharmacology, Medical College of Ohio, Toledo, OH 43614, USA

Received 12 November 2001; received in revised form 25 March 2002; accepted 25 March 2002

Abstract

Two days following one-week administration of the benzodiazepine, flurazepam (FZP), rats exhibit anticonvulsant tolerance *in vivo*, while reduced GABA_A receptor-mediated inhibition and enhanced EPSP amplitude are present in CA1 pyramidal neurons *in vitro*. AMPA receptor (AMPA)-mediated synaptic transmission in FZP-treated rats was examined using electrophysiological techniques in *in vitro* hippocampal slices. In CA1 pyramidal neurons from FZP-treated rats, the miniature excitatory postsynaptic current (mEPSC) amplitude was significantly increased (33%) without change in frequency, rise time or decay time. Moreover, mEPSC amplitude was not elevated in dentate granule neurons following 1-week FZP treatment or in CA1 pyramidal neurons following acute desalkyl-FZP treatment. Regulation of AMPAR number was assessed by quantitative autoradiography with the AMPAR antagonist, [³H]Ro48-8587. Specific binding was significantly increased in stratum pyramidale of hippocampal areas CA1 and CA2 and in proximal dendritic fields of CA1 pyramidal neurons. Regulation of AMPAR subunit proteins was examined using immunological techniques. Neither abundance nor distribution of GluR1–3 subunit proteins was different in the CA1 region following FZP treatment. These findings suggest that enhanced AMPAR currents, mediated at least in part by increased AMPAR number, may contribute to BZ anticonvulsant tolerance. Furthermore, these studies suggest an interaction between GABAergic and glutamatergic systems in the CA1 region which may provide novel therapeutic strategies for restoring BZ effectiveness. © 2002 Elsevier Science Ltd. All rights reserved.

Keywords: flurazepam; tolerance; AMPA receptors; mEPSCs; CA1; excitatory synapses

1. Introduction

Benzodiazepines (BZs) are clinically useful anxiolytics, hypnotics and anticonvulsants, however their usefulness as anticonvulsants is limited by development of tolerance which occurs during prolonged administration. BZs are allosteric modulators of γ -aminobutyric acid type A receptors (GABARs) which increase the frequency of Cl⁻ channel opening and potentiate inhibitory responses in the central nervous system (Macdonald and Olsen, 1994). BZ tolerance has been extensively studied in GABAergic inhibitory systems, in particular, the hippocampus since it is often a locus for epileptic activity. Accordingly, changes in GABAR structure, function and

pharmacology, thought responsible for BZ tolerance, have been well described (Barnes, 1996).

Rats chronically treated with the BZ, flurazepam (FZP), show anticonvulsant tolerance *in vivo* (Rosenberg, 1995), while in *in vitro* hippocampal slices, CA1 pyramidal neurons are tolerant to the potentiating effects of BZs (Xie and Tietz, 1992; Zeng and Tietz, 1999). Postsynaptic GABAR function is decreased in CA1 pyramidal neurons from chronic FZP-treated rats (Zeng et al., 1995; Poisbeau et al., 1997; Zeng and Tietz, 1999) and is correlated with significant alterations in the expression of GABAR subunit mRNA and protein (Chen et al., 1999; Tietz et al., 1999). Interestingly, CA1 neurons from FZP-treated rats also display increased fast, monosynaptically-evoked excitatory postsynaptic potentials (EPSPs) and a GABAR-mediated depolarizing potential (Zeng et al., 1995), which has been shown to modulate *N*-methyl-D-aspartate (NMDA) receptor function (Staley et al., 1995). Together these findings suggest that both fast, α -amino-3-hydroxy-5-methyl-4-isoxazo-

* Corresponding author. Tel.: +1-419-383-4182; fax: +1-419-383-2871.

E-mail address: etietz@mco.edu (E.I. Tietz).

lepropionic acid (AMPA) receptor-mediated and slower NMDA receptor-mediated excitatory neurotransmission may be altered in CA1 pyramidal neurons following chronic FZP-treatment.

EPSPs in CA1 pyramidal neurons result from excitatory postsynaptic currents (EPSCs) generated by flow of cations (Na^+ , K^+ , Ca^{2+}) through glutamate-activated excitatory amino acid receptors. In CA1 pyramidal neurons, AMPARs are glutamate-gated ion channels with fast kinetics and mediate the fast component of the EPSP. The slow component of the EPSP is mediated by glutamate-gated NMDARs which demonstrate slow kinetics, high permeability to Ca^{2+} , and voltage-dependence. Both receptors are hetero-multimeric complexes composed of homologous subunit proteins (reviewed in Dingledine et al. (1999)). CA1 pyramidal neurons express high levels of GluR(1–3) subunits (Wenthold et al., 1996), whereas NMDARs are composed of NR2(A–D) subunits assembled with at least one NR1 subunit (Buller et al., 1994; Blahos and Wenthold, 1996).

As previous findings suggested the fast CA1 pyramidal neuron EPSP was altered as a function of chronic FZP treatment (Zeng et al., 1995), initial studies of excitatory amino acid receptor function were focused on AMPAR-mediated responses. Evidence for participation of AMPARs in BZ tolerance is limited (reviewed in Jackson et al. (2000)), however, a recent study demonstrated increased GluR1 subunit mRNA and protein in selective brain regions, notably the hippocampus, following chronic diazepam treatment (Izzo et al., 2001). Moreover, several studies have demonstrated a role for AMPARs in tolerance and dependence associated with other drugs of abuse for which AMPARs are not the site of drug action (ethanol: Karczkubicha and Liljequist, 1995; morphine: Kest et al., 1997).

This study addresses changes in AMPAR function and expression that may underlie the increased amplitude of fast EPSPs in CA1 pyramidal neurons after chronic BZ treatment. To assess the effect of 1-week FZP treatment and its associated changes in GABAR-mediated inhibition (Zeng et al., 1995; Zeng and Tietz, 1999) on fast, excitatory responses, AMPAR-mediated miniature excitatory postsynaptic currents (mEPSCs) were recorded from CA1 pyramidal and dentate granule neurons using whole-cell patch techniques in *in vitro* hippocampal slices. Quantitative receptor autoradiography was used to examine changes in the total number of hippocampal AMPARs following FZP treatment. As regulation of individual GABAR subunit proteins was correlated with decreased GABAR function in CA1 pyramidal neurons (Chen et al., 1999), alterations in AMPAR subunit proteins, which may relate to a change in AMPAR function, were also analyzed using quantitative immunohistochemistry and immunoblotting techniques. Portions of this manuscript have been published in abstract form, Society

for Neuroscience Abstracts 25: 969 (1999); 26: 1129 (2000).

2. Materials and methods

2.1. Drugs and reagents

Tetrodotoxin (TTX) was purchased from Alomone Laboratories (Jerusalem, Israel). APV (DL-2-amino-5-phosphonovaleric acid), DNQX (6,7-dinitroquinoxaline-2,3-dione), (+)-bicuculline methiodide (BMI), lidocaine *N*-ethyl bromide quaternary salt (QX-314), picrotoxin and FZP dihydrochloride were obtained from Research Biochemicals International division of Sigma-Aldrich Chemical Co. (St. Louis, MO). Desalkyl-FZP was from Hoffman–LaRoche Inc. (Nutley, NJ). The AMPAR antagonist, [^3H]Ro48-8587 was from Amersham–Pharmacia (Arlington Heights, IL), and quisqualic acid was obtained from Sigma–Aldrich. The chemiluminescent detection system (Super Signal™) and 1-Step NBT/BCIP (nitro-blue tetrazolium chloride/5-bromo-4-chloro-3'-indolylphosphate *p*-toluidine salt) were purchased from Pierce (Rockford, IL). The subunit-specific polyclonal GluR2 antibody (Petralia et al., 1997) was a generous gift from Dr. Robert Wenthold. Additional antibodies were purchased from commercial sources: polyclonal GluR1, GluR2/3 and monoclonal actin (Chemicon International, Temecula, CA); horseradish peroxidase (HRP)-linked anti-rabbit IgG, HRP-linked anti-mouse IgG, alkaline phosphatase (AP)-linked anti-rabbit IgG, AP-linked anti-mouse IgG (Santa Cruz Biotechnologies, Santa Cruz, CA), and biotinylated anti-rabbit IgG F(ab')₂ fragments (Boehringer Mannheim, Indianapolis, IN). All other chemicals were obtained from Sigma-Aldrich.

2.2. Benzodiazepine treatment

Experimental protocols involving the use of vertebrate animals were approved by the Medical College of Ohio, Institutional Animal Care and Use Committee (IACUC) and conformed to National Institutes of Health guidelines. One-week FZP treatment was carried out as previously established (Xie and Tietz, 1992; Zeng and Tietz, 1999). Briefly, following 2-day adaptation to the 0.02% saccharin vehicle, male Sprague–Dawley rats (Harlan, Indianapolis, IN) were offered FZP in 0.02% saccharin water for 1 week (100 mg/kg for 3 days, 150 mg/kg for 4 days) as their sole source of drinking water. Daily water consumption was monitored for each rat and used to adjust drug concentration so that the criterion dose (>100 mg/kg/week) of FZP was achieved. Using this protocol, rats are tolerant to BZ suppression of pentylenetetrazole-induced seizures (Rosenberg, 1995) but show no signs of spontaneous or precipitated withdrawal

(Tietz and Rosenberg, 1988). Matched control rats received only saccharin water. At the end of drug administration, rats were offered saccharin water for 2 days before animals were euthanized for hippocampal slice preparation or cryostat tissue sectioning. At this time point, residual BZ and metabolites are no longer detectable in hippocampus by radioreceptor assay (<3 ng FZP and metabolites/g hippocampus; Xie and Tietz (1992)). To determine whether changes in hippocampal slices were specific to chronic BZ treatment, an acute dose of the FZP active metabolite, desalkyl-FZP, was given to another group of rats. Two days before sacrifice, 2.5 mg/kg of desalkyl-FZP was administered by gavage in an emulsion of peanut oil, water and acacia (4:2:1). Food was removed 12 h prior to gavage. Control rats received an equivalent volume of emulsion vehicle. The single dose of desalkyl-FZP was previously demonstrated by radioreceptor assay to result in levels of BZ activity (0.57 μ M diazepam equivalents) similar to that found in the hippocampus of rats after 1-week FZP treatment (0.57 μ M diazepam equivalents) without a concomitant effect on GABAR-mediated inhibition (Xie and Tietz, 1992).

2.3. Electrophysiology

2.3.1. Hippocampal slices

Hippocampal slices (450 μ m) were prepared from FZP-treated and control rats as previously described (Zeng et al., 1995; Zeng and Tietz, 1999). Briefly, rats were decapitated and transverse hippocampal slices were prepared on a vibratome (Ted Pella, Inc., Redding, CA) in ice-cold, pregassed (95% O₂/5% CO₂) ACSF containing (in mM): NaCl, 119; KCl, 2.5; CaCl₂, 1.8; MgSO₄, 1.3; NaH₂PO₄, 1.25; NaHCO₃, 26; D-glucose, 10; pH 7.4. Slices were maintained at room temperature for \geq 1 h in gassed ACSF. During recording, slices were perfused at 2.5 ml/min with gassed ACSF at room temperature.

2.3.2. Electrophysiological recording

AMPA-mediated, action potential independent, mEPSCs were isolated from CA1 pyramidal neurons or dentate granule neurons in the presence of 1 μ M TTX, 10 μ M glycine and 30 μ M BMI (or 50 μ M picrotoxin) using whole-cell voltage-clamp techniques as previously described (Zeng and Tietz, 1999). Briefly, patch pipettes (5–9 M Ω), pulled from borosilicate capillaries (nonfilamented, 1.5 mm O.D., World Precision Instruments, Sarasota, FL) on a Flaming–Brown electrode puller (P-97, Sutter Instruments Co., Novato, CA), were filled with internal solution containing (in mM): Cs-glucuronate, 122.5; CsCl, 17.5; HEPES, 10; EGTA, 0.2; NaCl, 8; Mg-ATP, 2; QX-314, 2; pH 7.2 adjusted with CsOH. Cs⁺ was included to eliminate GABA_B-mediated events. Neurons were voltage-clamped ($V_h = -80$ mV)

in continuous mode (cSEVC) using an Axoclamp 2A amplifier (Axon Instruments Inc., Foster City, CA). Current output was low-pass filtered (10 kHz), DC-offset and amplified 10 000-fold. The signal was continuously monitored on-line (PCLamp 6.0 Software, Axon Instruments Inc.), digitized (Digidata 1200, Axon) and stored on VCR tape for later off-line analysis. Baseline mEPSC activity was recorded in each neuron for at least 5 min. Recorded events ≥ -4 pA, (~ 2.5 – $4\times$ greater than the baseline root mean square noise) with faster rise than decay were detected and averaged using the Mini Analysis Program (Synaptosoft Inc., Leonia, NJ). Peak mEPSC amplitude was measured from baseline. Decay kinetics and mEPSC amplitude were also estimated using a single exponential function: $[y(t) = a \cdot \exp(-t/\tau)]$.

2.4. Autoradiography and protein expression

2.4.1. Brain section preparation

Two-days following 1-week FZP treatment, control and FZP-treated rats were deeply anesthetized with 50 mg/kg, i.p. sodium pentobarbital and perfused through the heart with 100 ml 0.1 M phosphate buffered saline (PBS), pH 7.3. Brains were removed and rapidly frozen in isopentane (-70 °C) cooled by acetone/dry ice bath. Parasagittal cryostat cut sections (20 μ m) were thaw-mounted onto gelatin/chrome alum-coated slides and stored at -70 °C until used for autoradiographic binding or immunohistochemical studies.

2.4.2. Autoradiographic binding

Autoradiographic binding studies were performed using standard techniques (Mutel et al., 1998). To reduce endogenous glutamate ($<0.4\%$ of initial values, unpublished HPLC studies), sections were pre-incubated at room temperature 1×10 min in buffer: 50 mM K₂HPO₄/NaH₂PO₄, 200 mM NaCl, 1 μ M EDTA (pH 7.4), followed by 2×10 min in 50 mM Tris–HCl (pH 7.0) buffer. Slides were dried under cold air then incubated 1 h at 4 °C in 50 mM Tris–HCl (pH 7.0) containing 25 nM [³H]Ro48-8587 (specific activity, 53 Ci/mmol). Non-specific binding was determined in the presence of 1 mM quisqualic acid. Sections were washed 2×30 s and 1×1 min in Tris–HCl buffer (4 °C) then dipped in ddH₂O to remove unbound radioligand and reduce non-specific binding. Slides were rapidly dried under cold air, vapor-fixed with paraformaldehyde for 2 h at 80 °C under vacuum, and exposed to [³H]Hyperfilm (Amersham) for 3 days. Film was developed 2 min using D19 developer (Eastman Kodak Company, Rochester, NY) diluted 1:1 with ddH₂O, fixed until clear with Rapid Fixer (Kodak) and washed 30 min in H₂O.

2.4.3. Immunohistochemistry

FZP-treated and control rat brain sections were handled in parallel throughout all procedures, as described and validated (Huang et al., 1996; Chen et al., 1999). Sections were rapidly thawed and warmed to room temperature under vacuum. Brain sections were post-fixed in 4% paraformaldehyde for 8 min, then washed 3×5 min in PBS. Fixed tissue sections were blocked 1 h at room temperature with 10% normal goat serum (v/v) plus 0.01% Triton X-100 (v/v) in PBS prior to application of primary antibody (GluR1: 2 µg/ml or GluR2: 1 µg/ml) and incubated overnight at 4 °C. After 3×5 min washes in PBS, matched FZP-treated and control sections were incubated with biotinylated anti-rabbit IgG F(ab')₂ fragment (1:250 in PBS) for 1 h at room temperature. Sections were washed 3×5 min in PBS and incubated in avidin–biotin–peroxidase complex (1:100 v/v; Vector Laboratories, Burlingame, CA) for 1 h. Immunostaining was visualized in fresh 0.05% diaminobenzidine (DAB; Sigma) in PBS. Hydrogen peroxide (0.01%) was added immediately before the chromagen reaction was initiated. The DAB reaction was carried out for 1–2 min and was identical for FZP-treated and control sections. The reaction was stopped by 5 min wash in PBS followed by dehydration through 75, 95, and 100% ethanol (4 min each). Sections were cleared with xylene and coverslipped with Permount (Fisher, Pittsburgh, PA). Primary antibody was omitted from one section per experiment to serve as negative control.

2.4.4. Image analysis

2.4.4.1. Quantitative autoradiography Film images were measured using a computer-assisted image analysis system (Huang et al., 1996). A light box (Northern Light, Imaging Research, St. Catherines, Ontario, Canada) provided constant illumination. Light intensity was adjusted to provide optimal contrast on the exposed film and was held constant between FZP-treated ($n = 8$) and control images ($n = 8$). Images of the hippocampus were acquired by high resolution CCD camera (Sierra Scientific, Sunnyvale, CA) with the aid of NIH Image software (v. 1.59). Specific binding (total minus non-specific binding), expressed as pmol/mg protein, was estimated by linear regression analysis ($r^2 = 0.99$) of standard curves derived from grey level values over the same film exposed simultaneously to [³H]thymidine brain paste standards. With 3 day film exposure, non-specific binding was not visible, so film background grey level was subtracted from grey levels representing total binding to give specific [³H]Ro48-8587 binding. Data are expressed as mean±S.E.M. of specific binding values (pmol/mg protein) and were compared by MANOVA. Post hoc comparisons were made using the method of Scheffé, $p \leq 0.05$.

2.4.4.2. Quantitative immunohistochemistry As described previously (Chen et al., 1999), images of immunostained brain sections were acquired similarly as for quantitative autoradiography. Slides were placed on the light box, and light intensity was optimized and held constant for acquisition of DAB immunostaining density from both FZP-treated ($n = 8$) and control ($n = 8$) tissue sections. Background grey level over white matter, i.e. the corpus callosum immediately dorsal to the hippocampus was subtracted from the grey level value derived from the hippocampal regions of interest to determine specific immunostaining density. All data are expressed as mean±S.E.M. of raw grey level values. Regional variations in the distribution of subunit protein immunostaining were compared by MANOVA with post hoc comparisons using the method of Scheffé, $p \leq 0.05$.

2.4.5. Immunoblot analysis

Immunoblot analysis using GluR1, GluR2, GluR2/3 and actin antibodies was carried out in CA1 and DG regions of the hippocampus microdissected from additional groups of FZP-treated ($n = 6$) and control ($n = 6$) rats, sacrificed 2 days following treatment. Slices were prepared as for electrophysiology, except that four slices were cut, 750–1000 µm in thickness, from the dorsal hippocampus. CA1 and DG regions were microdissected on ice under a microscope (20×, A.O. Instr., Buffalo, NY). The dissected tissue was homogenized 20 strokes with a teflon pestle in 100 µl of 0.32 M sucrose in a Potter–Elvehjem homogenizer. Total homogenates were stored at –70 °C until used. For crude membrane preparation, total homogenates were centrifuged at 700g for 10 min at 4 °C. The supernatant (S1) was removed and spun at 10 000g for 20 min at 4 °C to separate membranes from cytosol. The supernatant (S2) was removed, and the pellet (P2) containing cellular membranes was resuspended in 0.32 M sucrose, aliquoted and stored at –70 °C until used. Quantitation of protein from total protein and P2 fractions was determined using the method of Lowry.

Either total protein or P2 fractions from each control and FZP-treated hippocampal homogenate derived from the CA1 or DG region, was applied to alternate lanes of an 8% sodium dodecyl sulfate-polyacrylamide gel. Protein was separated at 180 V for 1.5 h in a Mini-Protean 3® apparatus (Biorad, Hercules, CA). Molecular weights of protein samples were estimated from pre-stained standards (14 300–200 000; Gibco-BRL, Gaithersburg, MD). Proteins were transferred to nitrocellulose membrane overnight at 30 V in a Mini Trans-Blot® apparatus (Biorad). The membrane was blocked 1 h at room temperature in 5% non-fat dry milk with Tris-buffered saline plus 0.05% Tween-20 (TBST; Fisher Biotech, Pittsburgh, PA). The membrane was rinsed 2×5 min in TBST and co-incubated for 2 h with primary antibodies (GluR1: 0.5 µg/ml, GluR2: 0.5 µg/ml or GluR2/3: 0.25

$\mu\text{g/ml}$ and actin: 1:1000) in blocking solution with shaking. This was followed by 6×5 min rinses in TBST. Immunoreactivity on nitrocellulose was detected using anti-rabbit (GluR1, GluR2 and GluR2/3) or anti-mouse (actin) secondary antibodies conjugated to HRP or AP. The nitrocellulose membrane was incubated with HRP-linked or AP-linked secondary antibodies (1:5000 in blocking solution) for 1 h at room temperature, rinsed 6×5 min in TBST and developed using Supersignal™ or NBT/BCIP substrate. Initially, enhanced chemiluminescence (ECL) was performed using Supersignal™, however due to very strong GluR1, GluR2, and actin signals, the AP method was chosen for subsequent experiments because of greater relative control of the colorimetric reaction using direct visualization of the nitrocellulose.

The density of bands reflecting GluR1, GluR2, GluR2/3 or actin protein was quantified using a densitometer (Model GS-670, Biorad) and Molecular Analyst Software (v. 1.1, Biorad). Density, measured as transmittance (ECL) or reflectance (AP), was expressed as volume-adjusted optical density (OD/mm^2). Adjusted OD values, reflecting AMPAR subunit protein levels, were determined for each CA1 or DG homogenate. Individual values were normalized to the respective OD value representing actin protein within the same homogenate. The expressed ratio of GluR1, GluR2 or GluR2/3 OD to actin OD was used to adjust for artifacts arising from variability in protein determination or loading. The difference between the means of the ratios calculated from densitometric measures of protein levels from control ($n = 6$) and FZP-treated ($n = 6$) rats was analyzed using an independent Student's *t*-test with a significance level of $p \leq 0.05$.

3. Results

3.1. Electrophysiology

3.1.1. CA1 pyramidal neuron mEPSCs after 1-week FZP treatment

In initial studies, whole-cell patch-clamp recordings were made from CA1 pyramidal neurons in hippocampal slices from FZP-treated (124 ± 5.3 mg/kg/week) and control adult rats (CON: 265.4 ± 4.6 g; FZP: 255.0 ± 6.6 g, final weight). In subsequent studies with juvenile rats (CON: 153.7 ± 4.9 g; FZP: 145.0 ± 4.2 g), results of recordings from CA1 neurons in FZP-treated (137.8 ± 4.4 mg/kg/week) and control rats were similar to that in adults, so data from adult and juvenile rats was pooled for further analysis. Resting membrane potential immediately after whole-cell acquisition (CON: -63.7 ± 1.7 mV, $n = 12$; FZP: -62.1 ± 1.6 mV, $n = 14$) was not significantly different between FZP-treated and control neurons. In the presence of TTX ($1 \mu\text{M}$), BMI

($30 \mu\text{M}$) and glycine ($10 \mu\text{M}$), spontaneous inward mEPSCs were observed in neurons voltage-clamped at -80 mV (Fig. 1A). These events were abolished by DNQX ($10 \mu\text{M}$) and unaffected by APV ($50 \mu\text{M}$) ($n = 3$; data not shown) indicating that, at -80 mV, mEPSCs represented AMPAR-mediated currents.

Averaged peak mEPSCs recorded in neurons from rats 2 days after 1-week FZP treatment were significantly increased in amplitude (CON: -8.9 ± 0.3 pA, $n = 12$; FZP: -12.1 ± 0.3 pA, $n = 14$; $p < 0.001$) when compared to those detected in control neurons (Fig. 1A). These values are in agreement with fitted amplitudes in Table 1. Consistent with this increase, the relative cumulative frequency distribution of mEPSC amplitudes (Fig. 2A) in CA1 neurons from FZP-treated and control rats showed a rightward shift. This reflects the significant (Kolmogorov–Smirnov, K–S, test, $p < 0.001$) increase in the proportion of larger amplitude events found in these neurons. The frequency of mEPSCs was not altered following 1-week FZP treatment (Table 1). Relative cumulative frequency distributions of mEPSC 10–90% rise time and decay time constant (τ) were constructed (Fig. 3A,B) to assess changes in macroscopic current properties. There were no significant differences in the 10–90% rise time or the decay time constant in neurons from FZP-treated rats relative to controls (K–S test, $p > 0.01$).

Since the amplitude and time-course of events recorded from pyramidal neurons can be distorted by dendritic filtering (Wyllie et al., 1994), plots of rise time and decay time constants versus amplitude were constructed for individual events. For all mEPSCs analyzed, there was no correlation between rise times and amplitudes (Fig. 3C) of events recorded in neurons from FZP-treated ($r^2 = 0.01$) and control ($r^2 = 0.01$) rats. There was only a weak correlation between decay time constants and amplitudes of events (Fig. 3D) recorded in neurons from FZP-treated ($r^2 = 0.19$) and control ($r^2 = 0.12$) rats. To determine if multiple populations of mEPSC event amplitudes exist in CA1 pyramidal neurons, mEPSC amplitude histograms were fit with gaussian functions. Individual CA1 pyramidal neurons from both control and FZP-treated rats could be best-fit with either two or three gaussian functions (Figs. 4A₁ and 4A₂), however, not all cells from the same treatment group could be best-fit with the same number of functions.

Amplitude histograms of the total number of mEPSCs recorded from neurons in slices from all control and FZP-treated rats were generated to compare populations of mEPSC amplitudes between treatment groups (Figs. 4A₃ and 4A₄). The amplitude histogram from control rats was best-fit ($df = 3,48$; $F = 35.57$; $p < 0.001$) with three gaussian functions (Fig. 4A₃; Mean₁ = -6.9 ± 0.1 pA, area under the curve (AUC)₁ =

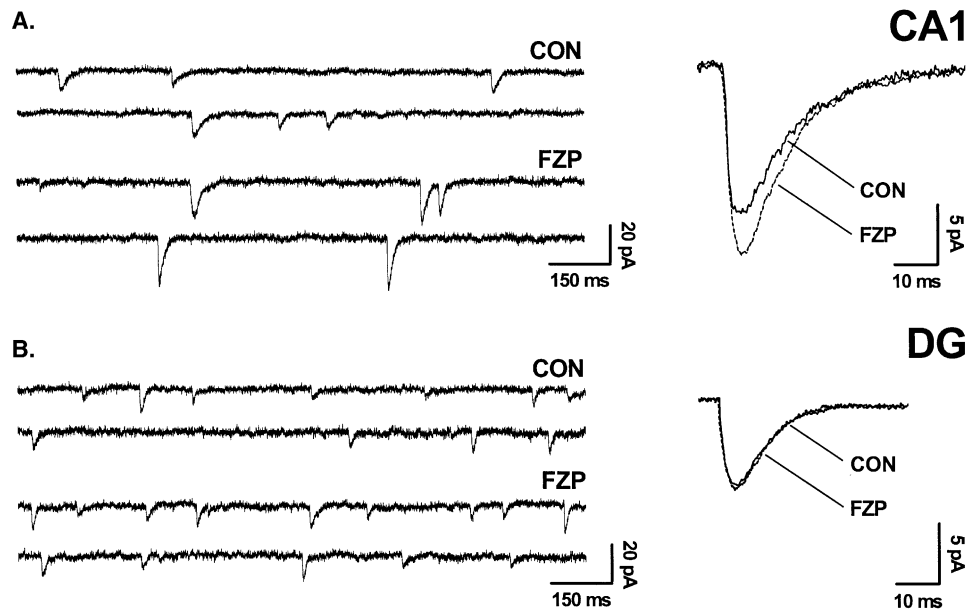


Fig. 1. AMPAR-mediated mEPSCs in hippocampal neurons from rats sacrificed 2 days after 1-week oral FZP treatment. (A) Representative traces of mEPSCs from individual CA1 neurons from control (top) and FZP-treated (bottom) rats recorded in the presence of 1 μ M TTX, 10 μ M glycine and 30 μ M BMI. Neurons from FZP-treated rats showed an increased mean mEPSC amplitude when compared to neurons from control rats. Right: Representative average mEPSC from a control CA1 neuron ($n = 83$ events) and a neuron from an FZP-treated rat ($n = 73$ events) different from those shown in traces. Following 1-week FZP treatment, there was a 33% increase in average mEPSC amplitude in CA1 pyramidal neurons relative to control neurons. (B) Representative traces of mEPSCs recorded from individual dentate granule neurons from control (top) and FZP-treated (bottom) rats recorded in the presence of 1 μ M TTX, 10 μ M glycine and 50 μ M picrotoxin. Right: Representative average mEPSC from a control dentate granule neuron ($n = 165$ events) and a neuron from an FZP-treated rat ($n = 193$ events) different from those shown in traces. There was no difference in average mEPSC amplitude in dentate granule neurons from FZP-treated rats relative to control neurons.

Table 1
mEPSC properties in hippocampal neurons from FZP-treated rats

Treatment (No. cells)	Rise time (ms)	Amplitude: a (pA) ^a	Decay: τ (ms)	Frequency (Hz)
Acute				
CA1 pyramidal neurons				
Control ($n = 5$)	3.4 \pm 0.2	-11.0 \pm 0.2	15.9 \pm 0.7	0.33 \pm 0.06
Desalkyl-FZP ($n = 5$)	3.5 \pm 0.3	-11.2 \pm 0.4	14.3 \pm 0.4	0.29 \pm 0.09
p value	0.97	0.98	0.46	0.92
Chronic				
CA1 pyramidal neurons				
Control ($n = 12$)	3.4 \pm 0.2	-10.4 \pm 0.5	15.6 \pm 0.7	0.29 \pm 0.05
1-week FZP ($n = 14$)	3.5 \pm 0.2	-13.8 \pm 0.4	14.6 \pm 0.7	0.25 \pm 0.05
p value	0.81	<0.001*	0.15	0.62
Dentate granule neurons				
Control ($n = 7$)	2.5 \pm 0.1	-6.7 \pm 0.2	10.1 \pm 0.7	0.77 \pm 0.12
1-week FZP ($n = 8$)	2.5 \pm 0.1	-7.0 \pm 0.2	9.7 \pm 0.5	0.95 \pm 0.12
p value	0.77	0.36	0.67	0.34

Values represent mean \pm S.E.M.

^a Amplitude (a) and decay (τ) values were derived from the best-fit of the equation: $[y(t) = a \cdot \exp(-t/\tau)]$.

* Significant difference ($p \leq 0.001$) between chronic control and FZP-treated groups by MANOVA with post hoc comparisons by the method of Scheffé.

270 \pm 112; Mean₂ = -9.7 \pm 0.6 pA, AUC₂ = 393 \pm 267; Mean₃ = -14.8 \pm 2.9 pA, AUC₃ = 288 \pm 182). Events of smaller amplitude were clearly decreased in CA1 neurons from FZP-treated rats, and the amplitude histogram of mEPSCs was best-fit

($df = 3,51$; $F = 15.49$; $p < 0.001$) with two gaussian functions (Fig. 4A₄; Mean₁ = -9.2 \pm 0.2 pA, AUC₁ = 280 \pm 128; Mean₂ = -14.6 \pm 1.1 pA, AUC₂ = 696 \pm 141).

3.1.2. CA1 pyramidal neuron mEPSCs after acute desalkyl-FZP treatment

Two days after a single dose of desalkyl-FZP (2.5 mg/kg p.o.) or control emulsion, whole-cell patch recordings were made in slices from acutely treated (140.3±8.3 g) and control (144.0±5.7 g) juvenile rats. Resting membrane potential immediately after whole-cell acquisition (CON: -61.8±2.1 mV, $n = 5$; desalkyl-

FZP: -64.8±3.1 mV, $n = 5$) was not different between neurons from control emulsion or acute desalkyl-FZP-treated rats. No significant differences in CA1 neuron mEPSC properties were detected between neurons following control emulsion or acute desalkyl-FZP treatment (CON: -9.7±0.2 pA, $n = 5$; desalkyl-FZP: -10.1±0.3 pA, $n = 5$; see also Table 1). Moreover, the properties of mEPSCs following acute treatment were not significantly different from those neurons from control rats offered saccharin water for 1 week. However, the mEPSC amplitude in CA1 neurons from 1-week FZP-treated rats was significantly greater ($p < 0.01$) than the mEPSC amplitude recorded in neurons from acute desalkyl-FZP treated and control emulsion-treated rats (MANOVA, $df = 3,22$; $F = 7.63$).

3.1.3. Dentate granule neuron mEPSCs after 1-week FZP treatment

Whole-cell patch-clamp recordings were made from dentate granule neurons in hippocampal slices from FZP-treated (135.8±3.6 mg/kg/week) and control juvenile rats (CON: 160.0±3.3 g; FZP: 150.8±4.1 g). Resting membrane potential immediately after whole-cell acquisition (CON: -63.0±2.0 mV, $n = 7$; FZP: -62.8±1.3 mV, $n = 8$) was not significantly different between granule neurons from FZP-treated and control rats. In the presence of TTX (1 μM), picrotoxin (50 μM) and glycine (10 μM), spontaneous inward mEPSCs were observed in neurons voltage-clamped at -80 mV (Fig. 1B). These events were abolished by DNQX (10 μM) and unaffected by APV (50 μM) (data not shown) indicating that, at -80 mV, mEPSCs represented AMPAR-mediated currents. Average mEPSCs recorded in neurons from rats 2 days after 1-week FZP treatment were not significantly increased in amplitude (CON: -6.2±0.2 pA, $n = 7$; FZP: -6.4±0.2 pA, $n = 8$) when compared

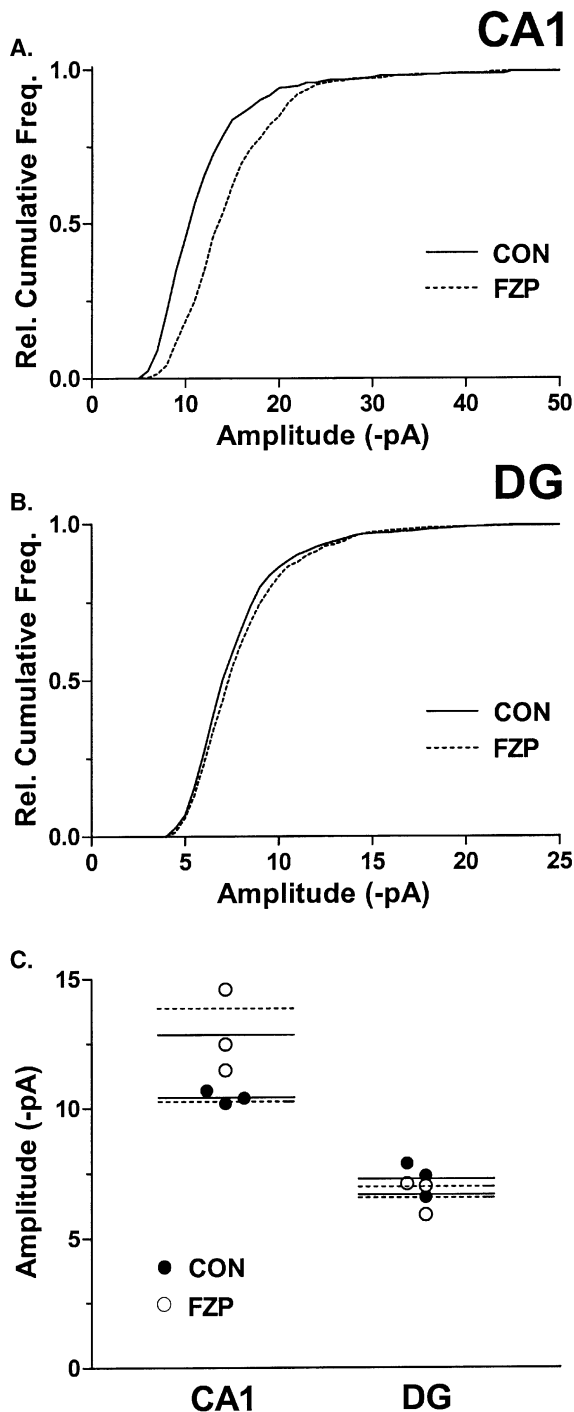


Fig. 2. Effects of chronic BZ treatment on mEPSC amplitude in hippocampal neurons from rats sacrificed 2 days after 1-week oral FZP treatment. (A) Relative cumulative frequency distribution of mEPSC amplitudes in CA1 neurons from control ($n = 12$) and FZP-treated ($n = 14$) rats. The distribution of mEPSC amplitudes in CA1 neurons from FZP-treated rats was significantly shifted to the right indicating a significant increase in the proportion of larger amplitude events (K-S test; $p < 0.001$). (B) Relative cumulative frequency distribution of mEPSC amplitudes in dentate granule neurons from control ($n = 7$) and FZP-treated ($n = 8$) rats. The distribution of mEPSC amplitudes in neurons from FZP-treated rats was not significantly different from control neurons (K-S test; $p > 0.01$). (C) Plot of mEPSC amplitudes in CA1 pyramidal and dentate granule neurons recorded in separate slices prepared from the same animal ($n = 3$ for both control and FZP-treated animals). In CA1 pyramidal neurons, the average mEPSC amplitude (—) in FZP-treated neurons (○) was significantly elevated (+28%, $p < 0.05$) relative to control (●) neurons, and this increase was similar to that observed (+33%) for the average amplitudes of all CA1 pyramidal cells recorded (- - -). In dentate granule neurons, the average mEPSC amplitudes (—) of control (●) and FZP-treated (○) neurons was similar to the averages found for all granule neurons recorded (- - -).

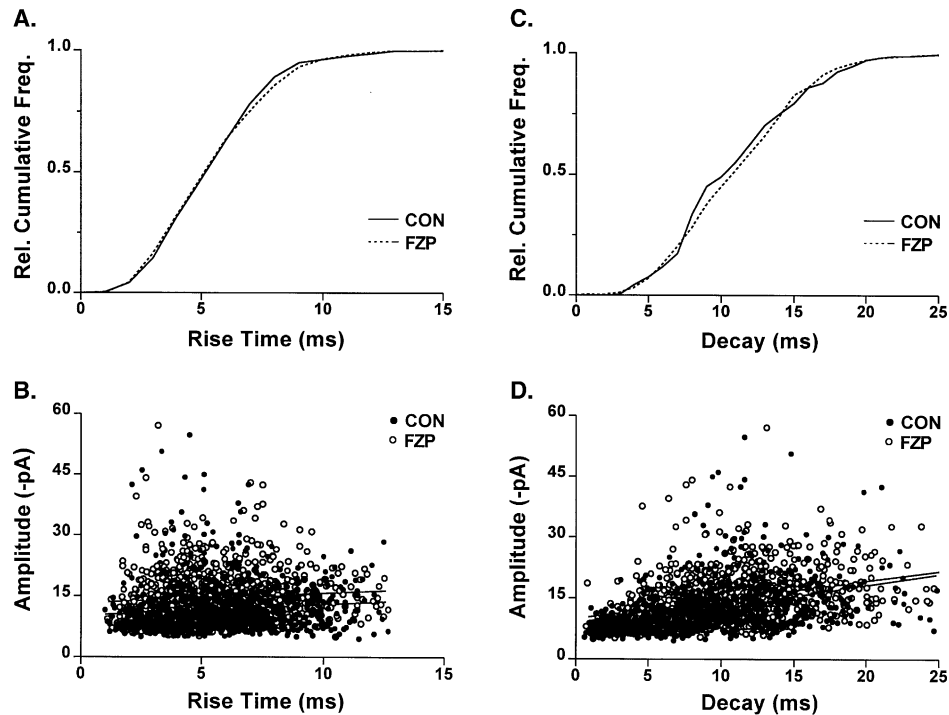


Fig. 3. Effects of chronic BZ treatment on mEPSC rise time and decay time constants in CA1 pyramidal neurons from rats sacrificed 2 days after 1-week oral FZP treatment. A, B: Relative cumulative frequency distributions of mEPSC rise times (A) and decay time constants (B) in CA1 pyramidal neurons from control ($n = 12$) and FZP-treated ($n = 14$) rats. There were no significant differences in the rise time or decay time constant in FZP-treated neurons relative to control neurons. (C, D) Plots of mEPSC rise time (C) and decay time constant (D) versus amplitude for individual events recorded in all control neurons ($n = 974$ events) and all neurons from FZP-treated ($n = 1004$ events) rats. There was no correlation between the rise time and the amplitude (C) of individual events recorded in CA1 neurons from control ($r^2 = 0.01$) or FZP-treated ($r^2 = 0.01$) rats. There was a small correlation between the decay time constant and the amplitude (D) of individual events recorded from control ($r^2 = 0.12$) and FZP-treated ($r^2 = 0.19$) neurons.

to those detected in control neurons (Table 1; Fig. 1B). The relative cumulative frequency distribution of mEPSC amplitudes (Fig. 2B) in dentate granule neurons from FZP-treated and control rats was not shifted toward larger amplitude events as was evident in CA1 pyramidal neurons. Changes in other macroscopic current properties of granule neurons were also not detected (Table 1). Similarly to CA1 pyramidal neurons, plots of rise time and decay time constants versus amplitude were constructed for dentate granule neuron mEPSCs (data not shown). No correlation was found between individual event rise times and amplitudes (CON: $r^2 = 0.01$; FZP: $r^2 = 0.00$), and only a weak correlation was found between individual event decay times and amplitudes (CON: $r^2 = 0.18$; FZP: $r^2 = 0.21$). This suggests that dendritic filtering was not affecting mEPSCs recorded in dentate granule neurons. The mEPSC amplitude histograms for dentate granule neurons from control and FZP-treated rats were generated to examine different populations of mEPSC amplitudes contributing to the average event amplitude (Fig. 4B₁ and B₂). The amplitude histogram from control neurons was best-fit (df = 3,120; $F = 62.15$; $p < 0.001$) with three gaussian functions (Mean₁ = -5.9 ± 0.1 pA, AUC₁ = 208 ± 12.7 ; Mean₂ =

-8.1 ± 0.1 pA, AUC₂ = 62.6 ± 7.8 ; Mean₃ = -9.7 ± 0.6 pA, AUC₃ = 82.5 ± 18.4). The amplitude histogram of mEPSCs from FZP-treated rats was also best-fit (df = 3,49; $F = 14.68$; $p < 0.001$) with three gaussian functions (Mean₁ = -5.6 ± 0.1 pA, AUC₁ = 146 ± 152 ; Mean₂ = -7.3 ± 0.8 pA, AUC₂ = 252 ± 235 ; Mean₃ = -10.9 ± 3.1 pA, AUC₃ = 100 ± 106). In a small group of control and FZP-treated rats, CA1 pyramidal and dentate granule neuron mEPSCs were recorded in separate slices prepared from the same animal (Fig. 2C). The average mEPSC amplitude recorded in CA1 pyramidal neurons from FZP-treated rats (-12.8 ± 0.9 pA, $n = 3$) was significantly ($p < 0.05$) elevated relative to control CA1 neurons (-10.1 ± 0.1 pA, $n = 3$). Moreover, this increase (28%) was similar to that observed for the total population of CA1 pyramidal neurons examined (+33%, Table 1). However, the average granule neuron mEPSC amplitudes (CON: -6.9 ± 0.4 pA; FZP: -6.7 ± 0.4 pA; $n = 3$ /group) recorded from the subset of cells were not different from each other nor from the total population of granule neurons studied (Table 1).

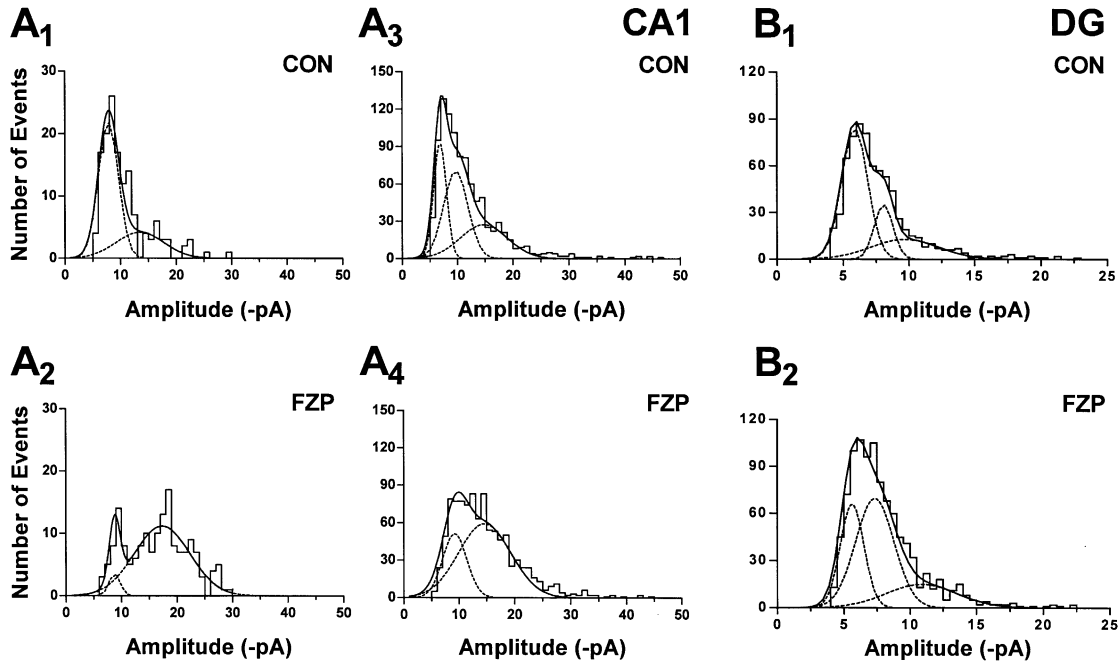


Fig. 4. Effects of chronic BZ treatment on mEPSC amplitude populations in hippocampal neurons from rats sacrificed 2 days after 1-week oral FZP treatment. (A) Histograms of mEPSC event amplitudes in CA1 pyramidal neurons. A₁, A₂, Representative amplitude histograms from individual CA1 pyramidal neurons from control (144 events) and FZP-treated (171 events) rats. Both amplitude histograms were best-fit with two gaussian functions (—). The individual functions (---) which comprised the best-fit had mean amplitudes of -7.8 ± 0.2 and -13.5 ± 4.0 pA in the control neuron (A₁) and -8.8 ± 0.2 and -17.3 ± 0.5 pA in the FZP-treated neuron (A₂). A₃, A₄, Amplitude histograms of the total population of CA1 pyramidal neurons from control (974 events, $n = 12$) and FZP-treated (1004 events, $n = 14$) rats. The control mEPSC population (A₃) was best-fit by three gaussian functions (—). Individual functions (---) had mean amplitudes of -6.9 ± 0.1 , -9.7 ± 0.6 , and -14.8 ± 2.9 pA. The FZP-treated mEPSC population (A₄) was best-fit with two gaussian functions (—). Individual functions (---) had mean amplitudes of -9.2 ± 0.2 , and -14.6 ± 1.1 pA. (B) Histograms of mEPSC event amplitudes in dentate granule neurons. B₁, B₂, Amplitude histograms from the total population of granule neurons from control (720 events, $n = 7$) and FZP-treated (1000 events, $n = 8$) rats. Both granule neuron mEPSC populations were best fit with three gaussian functions (—). Individual functions (---) in control neurons (B₁) had mean amplitudes of -5.9 ± 0.1 , -8.1 ± 0.1 , and -9.7 ± 0.7 pA. Individual functions (---) in FZP-treated neurons (B₂) had mean amplitudes of -5.6 ± 0.1 , -7.3 ± 0.8 , and -10.9 ± 3.1 pA.

3.2. Quantitative autoradiography

The total number of hippocampal AMPARs was investigated by quantitative receptor autoradiography using a saturating concentration (25 nM) of ligand. Comparison of sections from control and FZP-treated rats indicated a significant increase in specific [³H]Ro48-8587 binding in several hippocampal regions 2 days after 1-week FZP treatment (Table 2, Fig. 5).

Significant increases in specific binding were detected in stratum pyramidale of the CA1 (+23.4%) and CA2 (+29.2%) regions. There was a trend toward increased binding in stratum oriens and radiatum of area CA2, stratum pyramidale of CA3 and the granule cells of dentate gyrus. Since pyramidal neurons possess recurrent axon collaterals that can directly activate their proximal dendritic regions (Crépel et al., 1997), measurements were also made in proximal dendritic regions immediately adjacent to the CA1, CA2 and CA3 pyramidal cell bodies. These measurements indicated increased specific binding in the proximal dendrites of stratum oriens (+11.2%) and stratum radiatum (+11.1%) of the CA1 region in control versus FZP-treated rats, while no dif-

ferences were found in proximal dendritic regions of area CA2 or CA3.

3.3. Quantitative immunohistochemistry

The relative GluR1 and GluR2 subunit antibody immunostaining patterns in the hippocampus observed in this study (Fig. 6A,B) were similar to those described previously using both light microscopic and electron microscopic techniques (Petralia and Wenthold, 1992; Petralia et al., 1997). The intensity of AMPAR subunit immunostaining density over several hippocampal regions was compared in sections derived from FZP-treated and control rats to determine the relative amount of each antigen present (Table 3).

A significant ($p < 0.05$) effect of FZP-treatment was found (MANOVA, $df = 1,321$; $F = 4.53$) and post hoc analysis detected a significant increase in GluR1 subunit immunostaining density in the proximal dendritic region of CA2 pyramidal neurons in stratum oriens (+16.2%). Significant changes were not detected in any other hippocampal region in FZP-treated rats (Fig. 6A). For the AMPAR GluR2 subunit, small, significant decreases in

Table 2
25 nM [³H]Ro48-8587 binding in hippocampus

	CA1					CA2				
	SO	SO-P	SP	SR-P	SR	SO	SO-P	SP	SR-P	SR
Control	17.3±0.5	16.8±0.6	12.4±0.7	16.9±0.5	18.8±0.8	12.7±0.4	14.5±0.6	7.3±0.5	15.4±0.5	14.0±0.5
FZP-treated	18.2±0.4	18.7±0.2	15.3±0.3	18.8±0.4	20.3±0.6	13.8±0.4	14.4±0.9	9.4±0.5	15.3±0.9	15.4±0.5
% from control	5.4	11.2	23.4	11.1	8.0	8.5	-1.3	29.2	-0.4	10.0
<i>p</i> value	0.14	< 0.01 **	< 0.01 **	< 0.01 **	0.13	0.07	0.85	< 0.01 **	0.95	0.06

	CA3					DG		
	SO	SO-P	SP	SL-P	SL	MOL	GC	PC (CA4)
Control	14.1±0.4	13.1±0.5	8.6±0.4	14.0±0.9	15.4±0.5	15.7±0.3	5.5±0.3	11.4±0.5
FZP-treated	14.0±0.4	13.5±0.5	9.4±0.2	14.5±0.5	15.8±0.5	16.1±0.5	6.3±0.4	12.4±0.5
% from control	-0.7	2.9	9.8	3.3	2.8	2.9	14.4	8.3
<i>p</i> value	0.84	0.58	0.08	0.62	0.56	0.40	0.10	0.13

Mean (±S.E.M.) pmoles/mg protein.

** Significant difference ($p \leq 0.01$) between control and FZP-treated groups; control: $n = 8$; FZP-treated: $n = 8$. CA1–CA3: SO, stratum oriens; SO-P, stratum oriens proximal dendrites; SP, stratum pyramidale; SR-P, stratum radiatum proximal dendrites; SR, stratum radiatum; SL, stratum lucidum; SL-P, stratum lucidum proximal dendrites; Dentate: MOL, molecular layer; GC, granule cells; polymorph (CA4) cells; PC, polymorph (CA4) cells.

immunostaining density were detected in the molecular layer (-6.0%) and granule cells (-4.3%) of the dentate gyrus (Fig. 6B), however, these small changes are near the limit of sensitivity of this technique (Huang et al., 1996). Differences in GluR2 immunostaining density were not detected in the cellular or dendritic layers of any other hippocampal region 2 days following the end of FZP treatment. Although appreciable levels of GluR3 subunit mRNA and protein are present in hippocampus (Wenthold et al., 1996; Izzo et al., 2001), GluR3 subunit protein was not examined due to the lack of a subunit specific antibody.

3.4. Immunoblot analysis

AMPA subunit proteins were studied in hippocampal homogenates of areas CA1 and dentate gyrus prepared as described in the Materials and Methods. For FZP-treated ($n = 6$) and control rats ($n = 6$), a total protein or a crude P2 fraction from areas CA1 and DG was examined for GluR1, GluR2, GluR2/3 and actin protein using quantitative immunoblot techniques. A band of 106–108 kD was detected using anti-GluR1, anti-GluR2 and anti-GluR2/3 subunit specific antibodies. The anti-actin antibody recognized a single band of 42 kD. Single bands at the appropriate molecular weight were detected using both enhanced chemiluminescence and AP-NBT/BCIP detection systems (Fig. 7A,C). The densities of the AMPAR subunit bands were expressed as a ratio relative to the density of the actin band within the same sample.

No significant differences in GluR1 (Fig. 7B) or

GluR2 (Fig. 7D) subunit protein were detected in CA1 or DG total protein derived from FZP-treated versus control rats. As movement of receptors from cytoplasmic to membrane locations is a potential mechanism for AMPAR regulation (Shi et al., 1999), the abundance of GluR1 and GluR2 subunit proteins was also examined in a neuronal membrane preparation. In P2 fractions prepared from areas CA1 or DG, no significant differences in the abundance of GluR1 (Fig. 7B) or GluR2 (Fig. 7D) subunit protein were detected between FZP-treated and control rat groups. As GluR2 subunit protein levels were not changed in areas CA1 or DG following FZP treatment, a GluR2/3 subunit specific antibody was used in the absence of an adequate GluR3 subunit specific antibody to assess changes in GluR3 subunit protein. No change in the abundance or distribution of GluR2/3 subunit protein was detected in the CA1 region or DG by immunoblot analysis (data not shown).

4. Discussion

The functional and receptor binding analysis of AMPARs in this study supports the hypothesis that chronic *in vivo* regulation of GABARs by BZs is associated with an upregulation of excitatory amino acid receptors in hippocampal CA1 pyramidal neurons. Using a treatment protocol that reliably and selectively decreases GABAergic function (Zeng et al., 1995; Poisbeau et al., 1997; Zeng and Tietz, 1999) and regulates GABAR subunit mRNA and protein (Tietz et al., 1999; Chen et al., 1999) in CA1 pyramidal neurons, the present

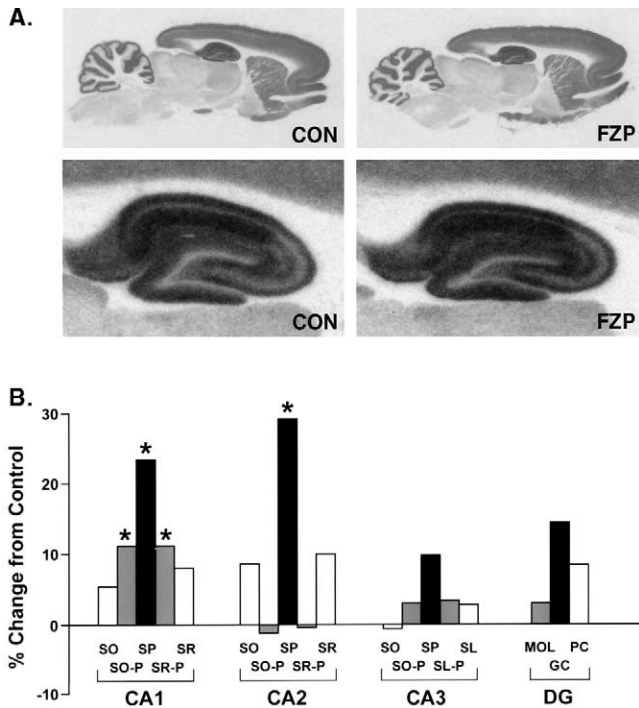


Fig. 5. AMPAR antagonist [³H]Ro48-8587 binding is increased in selective hippocampal subregions of the hippocampus in rats sacrificed 2 days after 1-week oral FZP treatment. Parasagittal brain sections (20 μm) were cut from control and FZP-treated rats 2 days following 1-week treatment. Sections were incubated with a saturating concentration (25 nM) of [³H]Ro48-8587 and exposed to [³H] sensitive film for 3 days. (A) Representative images of total [³H]Ro48-8587 binding in whole brain (top) and hippocampus (bottom) from control (CON) and FZP-treated (FZP) rats. Since non-specific binding, in the presence of 1 mM quisqualic acid, was not apparent with 3 day film exposure, images represent specific binding. (B) Quantification of specific [³H]Ro48-8587 binding in hippocampal subregions from FZP-treated rats expressed as percentage change from control specific binding. Significant increases in [³H]Ro48-8587 binding were detected in stratum pyramidale (SP) of areas CA1 and CA2, and in the proximal dendrites of CA1 pyramidal neurons (SO-P, SR-P) in area CA1, but not in area CA2 or CA3. No significant changes in [³H]Ro48-8587 binding were found in any other hippocampal subregion analyzed. Asterisks denote significant differences between control and FZP-treated mean (± S.E.M.) specific binding values, $p \leq 0.01$.

study detected a significant increase in postsynaptic AMPAR-mediated function in this same neuron population. This enhancement was not found following acute BZ treatment or in dentate granule neurons following chronic BZ treatment. Furthermore, spatially restricted increases in total AMPAR number were found to provide an anatomical basis for the observed increase in excitatory function. Regulation of AMPAR function and number following chronic BZ exposure suggests excitatory amino acid receptors may contribute to BZ anti-convulsant tolerance. Alternately, coupled with the findings of others (Steppuhn and Turski, 1993; Izzo et al., 2001), increased AMPAR function may signal an emerging physiological mechanism underlying signs of BZ withdrawal and dependence.

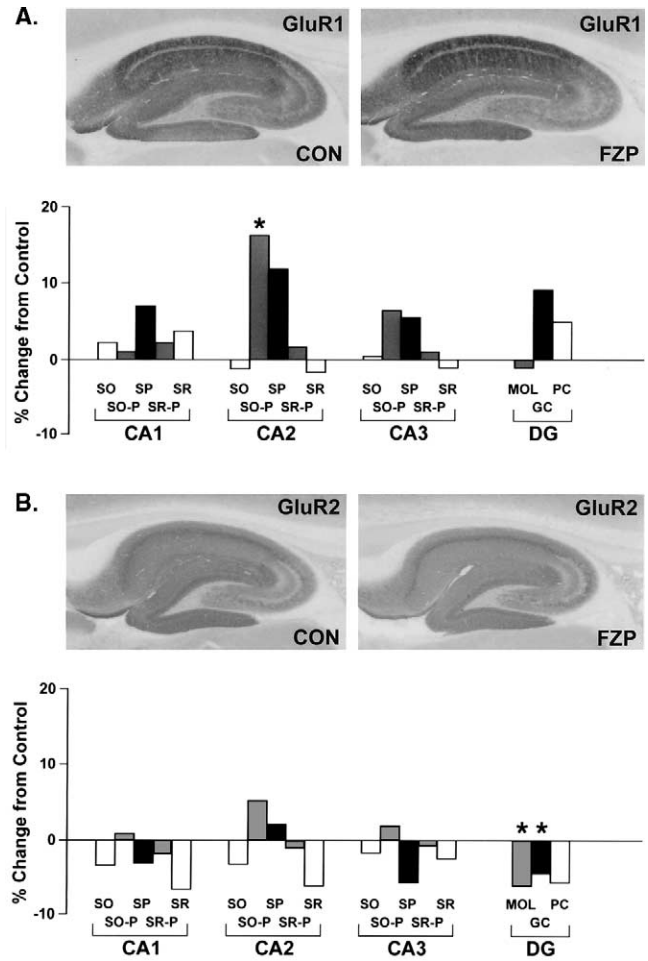


Fig. 6. Levels of AMPAR subunits GluR1 and GluR2 immunostaining in selective subregions of the hippocampus in rats sacrificed 2 days after 1-week oral FZP treatment. Brain sections (20 μm) from control and FZP-treated rats were immunostained with GluR1 or GluR2 subunit specific antibodies. Regional variations in immunohistochemical staining were examined using computer-assisted image analysis. Immunostaining density was compared in several hippocampal subregions between control and FZP-treated rats prepared 2 days after 1-week FZP treatment. (A, top) Relative distribution of GluR1 immunostaining in representative sections from control (CON) and FZP-treated (FZP) rats. (A, bottom) Quantification of GluR1 immunostaining density in hippocampal subregions from FZP-treated rats expressed as percentage change from control. A significant increase in relative grey level was detected in the proximal dendritic region of pyramidal neurons in stratum oriens (SO-P) of area CA2. Significant differences in GluR1 immunostaining density were not detected between FZP-treated and control rats in any other hippocampal region. (B, top) Relative distribution of GluR2 immunostaining in representative sections from control (CON) and FZP-treated (FZP) rats. (B, bottom): Quantification of GluR2 immunostaining density in hippocampal subregions from FZP-treated rats expressed as percent change from control. Significant decreases in relative grey level were detected in the molecular layer (MOL) and granule cells (GC) of the dentate gyrus. No significant differences between FZP-treated and control rats were detected for GluR2 immunostaining density in any other hippocampal subregion. Asterisks denote significant differences in mean (±S.E.M.) relative grey level values between brain sections from control and FZP-treated rats, $p \leq 0.05$.

Table 3
GluR1 and GluR2 subunit antibody immunostaining in hippocampus

GluR1	CA1					CA2				
	SO	SO-P	SP	SR-P	SR	SO	SO-P	SP	SR-P	SR
Control	37.8±1.9	38.3±1.7	30.2±2.1	37.4±1.7	35.6±1.8	34.4±2.0	32.0±1.8	29.2±2.2	36.1±1.8	34.3±1.7
FZP-treated	38.6±2.4	38.8±1.8	32.4±1.0	38.2±1.8	37.0±2.2	34.0±1.5	37.2±1.6	32.7±2.1	36.7±1.8	33.7±1.8
% from control	2.2	1.1	7.1	2.2	3.7	-1.2	16.2	11.9	1.6	-1.6
<i>p</i> value	0.78	0.86	0.35	0.73	0.63	0.87	<0.05*	0.24	0.81	0.81
GluR2	CA3					DG				
	SO	SO-P	SP	SL-P	SL	MOL	GC	PC(CA4)		
Control	27.5±1.0	26.7±1.0	20.2±0.9	26.8±1.0	25.8±1.0	33.9±1.3	26.5±1.2	25.6±0.9		
FZP-treated	27.6±1.8	28.4±1.7	21.3±1.3	27.1±1.3	25.6±1.3	33.6±1.4	28.9±1.1	27.2±1.2		
% from control	0.4	6.5	5.6	1.0	-1.1	-1.0	9.1	4.9		
<i>p</i> value	0.96	0.36	0.45	0.87	0.86	0.88	0.16	0.36		
GluR1	CA1					CA2				
	SO	SO-P	SP	SR-P	SR	SO	SO-P	SP	SR-P	SR
Control	36.6±1.3	41.0±0.9	46.5±1.0	42.9±0.7	38.2±1.4	35.0±1.5	37.0±0.9	42.8±1.0	38.6±0.8	35.4±1.2
FZP-treated	35.4±0.6	41.4±1.0	45.1±0.7	42.1±1.0	35.7±0.5	33.9±0.5	14.4±0.9	43.7±0.8	38.2±0.7	33.3±0.6
% from control	-3.3	0.9	-3.0	-1.8	-6.4	-3.1	5.3	2.1	-1.1	-6.0
<i>p</i> value	0.34	0.79	0.23	0.50	0.08	0.45	0.12	0.46	0.69	0.10
GluR2	CA3					DG				
	SO	SO-P	SP	SL-P	SL	MOL	GC	PC(CA4)		
Control	32.2±0.9	35.9±0.8	22.7±0.8	32.1±0.6	28.5±0.8	41.5±0.8	42.2±0.5	33.5±0.9		
FZP-treated	31.6±0.7	36.6±1.3	21.5±0.7	31.9±1.0	27.9±0.8	39.0±0.7	40.4±0.7	31.6±0.9		
% from control	-1.7	1.9	-5.5	-0.8	-2.4	-6.0	-4.3	-5.6		
<i>p</i> value	0.63	0.6	0.22	0.82	0.53	<0.05*	<0.05*	0.13		

Mean (±S.E.M.) relative grey values.

* Significant difference ($p \leq 0.05$) between control and FZP-treated groups; control, $n = 8$; FZP-treated, $n = 8$. CA1–CA3: SO, stratum oriens; SO-P, stratum oriens proximal dendrites; SP, stratum pyramidale; SR-P, stratum radiatum proximal dendrites; SR, stratum radiatum; SL, stratum lucidum; SL-P, stratum lucidum proximal dendrites; dentate: MOL, molecular layer; GC, granule cells; polymorph(CA4) cells PC, polymorph (CA4) cells.

4.1. Electrophysiology

While impairment of GABAR-mediated inhibitory function plays a well-established role in expression of BZ tolerance, the increased AMPAR-mediated mEPSC amplitude detected in CA1 pyramidal neurons from FZP-treated rats may provide an additional physiological mechanism for reduced BZ effectiveness. Regulation of postsynaptic AMPAR-mediated mEPSCs could arise from changes in the physiological properties of synaptic AMPARs as well as from changes in the number of functional AMPARs present at CA1 pyramidal neuron synapses. A significant increase in CA1 neuron mEPSC amplitude (Fig. 1A) was noted in the absence of changes in mEPSC frequency, rise time or decay time constant (Table 1), and dendritic filtering did not appear to differentially shape the properties

of mEPSCs in neurons from control or FZP-treated rats (Fig. 3). Increased mEPSC amplitude was not detected following acute desalkyl-FZP treatment, and moreover, increased mEPSC amplitude was not found in dentate granule neurons after 1-week FZP treatment suggesting a differential regulation of excitatory function in the hippocampus following chronic BZ treatment. This finding closely parallels the differential reduction in GABAergic inhibition found in the hippocampus following the same 1-week FZP treatment, i.e. reduced CA1 pyramidal neuron miniature inhibitory postsynaptic current (mIPSC) amplitude but not dentate granule neuron mIPSC amplitude (Poisbeau et al., 1997). Together, these findings suggest a role for decreased GABAR-mediated inhibition in regulation of postsynaptic excitatory receptor function in CA1 pyramidal neurons after chronic BZ exposure.

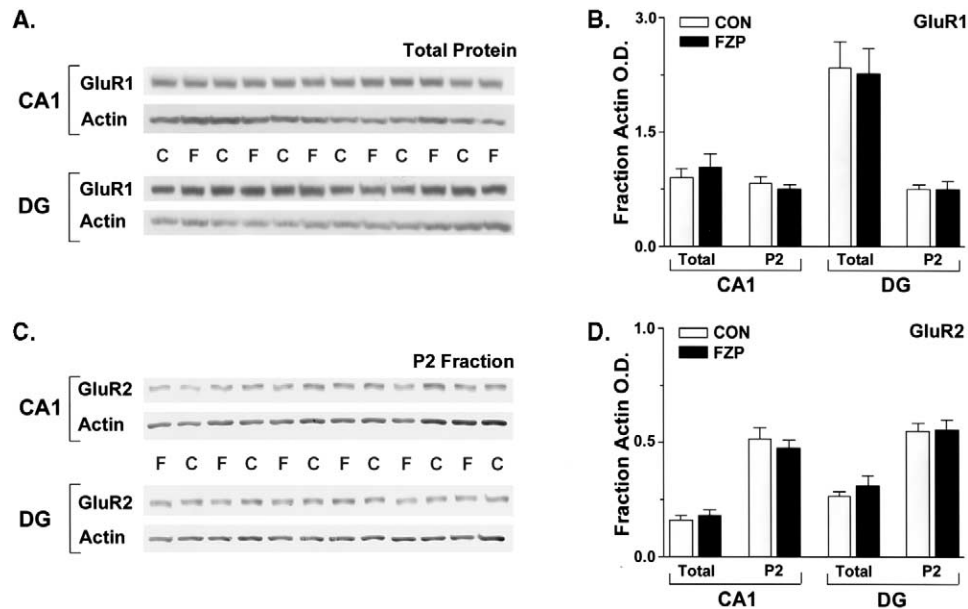


Fig. 7. The abundance of GluR1 and GluR2 AMPAR subunit proteins in hippocampal homogenates of area CA1 and dentate gyrus (DG) in rats sacrificed 2 days following 1-week oral FZP treatment. Crude homogenates were prepared from microdissected hippocampal subregions, CA1 and DG, and were fractionated further by centrifugation. Equal amounts of protein, (10 μ g, total protein; 5 μ g, P2 fraction) from control (C) and FZP-treated (F) rats were loaded per lane and separated by SDS-PAGE. After transfer to nitrocellulose, immunoblots were probed with antibodies specific for GluR1, GluR2, GluR2/3 (data not shown) and actin. Specific bands were visualized using enhanced chemiluminescence (ECL) or AP detection systems. (A) Representative immunoblots for total protein from regions CA1 and DG probed for the GluR1 subunit and actin and visualized with ECL. (B) Densitometric quantification of GluR1 subunit protein abundance in the total protein and P2 fractions from hippocampal homogenates of CA1 and DG. No significant differences in the levels of GluR1 subunit protein were detected in either the total or the P2 fraction derived from hippocampal CA1 or DG regions of FZP-treated as compared to control rats. (C) Representative immunoblots for the P2 fraction from regions CA1 and DG probed for the GluR2 subunit protein and actin and visualized with AP/NBT-BCIP substrate. (D) Densitometric quantification of GluR2 subunit protein abundance in total protein and P2 fractions from hippocampal homogenates of CA1 and DG. No significant differences in the levels of GluR2 subunit protein were detected between control and FZP-treated rats in either the total or the P2 fraction of hippocampal CA1 or DG regions.

Gaussian fits of mEPSC amplitude histograms in CA1 pyramidal neurons revealed three populations of amplitudes in control rats, while two populations were found in 1-week FZP-treated rats. Interestingly, the mEPSC amplitude histograms for dentate granule neurons from control and FZP-treated rats were both best-fit by three functions with remarkably similar mean amplitudes (Fig. 4). Loss of the lowest mean amplitude population in CA1 neurons from FZP-treated rats is consistent with the increased proportion of higher amplitude events found in these cells. These populations of mean amplitudes may represent:

1. distinct AMPAR populations with differing subunit composition (Wenthold et al., 1996) or functional properties, e.g. conductance (reviewed in Dingledine et al. (1999));
2. variation in synaptic AMPAR number (Nusser et al., 1998); or
3. AMPAR populations with different spatial distributions within the dendritic tree of CA1 neurons.

Following chronic FZP treatment, the increase in the

average mEPSC amplitude detected in CA1 pyramidal neurons may indicate changes in the number, subunit composition, distribution, or function of AMPAR populations. Macroscopic properties of mEPSCs, i.e. amplitude, rise-time and decay time constant, are subject to alteration by changes in the microscopic current properties of individual channels which contribute to the ensemble current. Indeed, regulation of AMPAR microscopic properties has been demonstrated to occur and to contribute to alterations in AMPAR-mediated responses following use-dependent changes in synaptic plasticity, i.e. long-term potentiation (Derkach et al., 1999). Interestingly, a shift in mEPSC amplitudes similar to that observed in this study was demonstrated in CA1 neurons following repetitive, postsynaptic depolarizations (Wyllie et al., 1994). Increased synaptic strength is, in part, related to a cascade of intracellular processes which results in regulation of synaptic AMPAR properties, including increases in synaptic receptor number (Shi et al., 1999) or channel conductance (Derkach et al., 1999). As the microscopic current properties of individual AMPARs could not be measured with the methods

employed in this study, it remains to be determined whether alterations in single-channel conductance or receptor kinetics may have also contributed to increased AMPAR-mediated mEPSC amplitude following chronic FZP treatment. Changes in AMPAR number or distribution that may have contributed to enhanced synaptic efficacy specific to CA1 pyramidal neurons were examined with AMPAR autoradiography and subunit protein expression studies.

4.2. Receptor binding autoradiography and protein expression

As glutamate is likely saturating at the postsynapse (Clements et al., 1992), changes in AMPAR affinity for glutamate are not likely responsible for enhanced AMPAR-mEPSC amplitude in CA1 neurons. Accordingly, a saturating concentration of ligand was used to examine AMPA receptor number in hippocampal regions following 1-week FZP treatment. A change in functional AMPAR number was suggested by the finding of localized increases in binding of the AMPAR antagonist, [³H]Ro48-8587, in areas CA1 and CA2 (Table 2 and Fig. 4). Increased AMPAR number was limited to the pyramidal cell layer and the proximal dendritic fields of CA1 pyramidal neurons. Pyramidal cell bodies are reported to lack excitatory synapses (Blackstad, 1963; Papp et al., 2001; R. Petralia, personal communication), however, pyramidal cell bodies are staggered throughout the width of the cell layer. Therefore, it is plausible that increased receptor numbers in proximal dendrites of some pyramidal cells may have contributed to the increased binding detected in the pyramidal cell layer.

A functional increase in synaptic AMPAR number could be attributed to increased receptor synthesis or to redistribution of receptors from intracellular to synaptic locations. Either of these mechanisms would allow increased AMPAR number to be reflected in increased postsynaptic AMPAR function. Quantitative immunohistochemical analysis indicated no significant alteration in abundance or localization of AMPAR subunit proteins in the CA1 region, and immunoblot analyses indicated no significant differences in total AMPAR subunit proteins in the CA1 region or dentate gyrus. Shi et al. (1999) demonstrated rapid insertion of AMPARs into the neuronal membrane following synaptic activation suggesting that shifts in cellular distribution of AMPARs may regulate synaptic receptor activity. This possibility was addressed by using cellular fractionation to prepare a neuronal membrane enriched fraction (Fig. 5). However, neither the amount of GluR1 nor GluR2 subunit protein within this P2 fraction was altered following BZ treatment. This latter finding suggests that increased number of AMPARs on the neuronal membrane may not underlie the increased mEPSC amplitude. However, small

shifts of AMPARs within cellular compartments of discrete, dendritic regions following FZP treatment may have occurred, yet was undetectable using immunoblot analysis of entire hippocampal regions. Further fractionation of subcellular compartments or utilization of higher resolution immunohistochemical techniques may be necessary to achieve the resolution required to detect such small, localized changes in synaptic receptor subunit proteins. Therefore, following chronic BZ treatment, the possibility of discrete, non-uniform changes in abundance or distribution of AMPAR subunit proteins within specific neuronal compartments of CA1 pyramidal neurons cannot be completely dismissed since such changes may not have been observed with the techniques available in this study.

4.3. Local circuitry of the CA1 region

Chronic FZP treatment resulted in upregulation of total AMPAR number within selected areas of the hippocampus. Restricted increases in binding suggest that spatial distribution of synaptic contacts onto CA1 neurons, e.g. versus onto dentate granule neurons, may be important in regulation of excitatory neurotransmission. In the CA1 region, two major systems of excitatory afferents contribute to the EPSP:

1. Schaffer collateral synaptic inputs; and
2. local circuit fibers which are collateral axons of pyramidal neurons (Bayazitov and Kleschevnikov, 2000).

Interestingly, blockade of GABA-mediated inhibition in the CA1 region revealed AMPAR- and NMDAR-mediated polysynaptic responses in proximal apical dendrites of CA1 pyramidal neurons driven by local recurrent collaterals (Crépel et al., 1997). Normally, the apical shaft of CA1 pyramidal cells is likely under tonic interneuron control (Papp et al., 2001), with suppression of local recurrent excitatory circuits by GABAergic inhibition. However, following FZP-treatment, postsynaptic GABAergic inhibition in CA1 pyramidal neurons was profoundly compromised, and decreased interneuron network activity in the CA1 region was suggested (Zeng et al., 1995; Zeng and Tietz, 1999). Therefore, substantial impairment of GABAergic inhibitory function in the CA1 region following 1-week FZP treatment may have permitted altered levels of local excitation. Such a mechanism can occur in pathologies such as epilepsy, where local recurrent excitatory connections are unmasked by degeneration of interneurons (Houser and Escalapez, 1996). Indeed, decreased perisomatic mIPSC activity (Hirsch et al., 1999) promotes increased basal excitatory synaptic drive onto CA1 pyramidal neurons (Escalapez et al., 1999). Chronic BZ treatment may permit a similar, yet more subtle disinhibition of local excitatory connections in the CA1 region. After 1-week FZP adminis-

tration, decreased network inhibition with subsequent enhanced excitatory drive onto proximal dendritic regions of CA1 pyramidal neurons may have contributed to plasticity in a discrete, local population of AMPARs. Dentate granule neurons, in which GABAR-mediated inhibition is not compromised (Poisbeau et al., 1997), do not exhibit similar plasticity (Table 1, Fig. 2B).

4.4. Homeostatic plasticity and dependence

Few studies have examined the effect of decreased GABAergic inhibition to modulate excitatory receptor function, yet the converse has been widely demonstrated. *In vitro*, modulation of excitatory activity by antagonists or agonists alters GABAR function as well as subunit mRNA and protein expression (Zhu et al., 1995; Gault and Siegel, 1998; Wang et al., 1998). *In vivo*, Matthews et al. (2000) established that 2-week blockade of NMDARs with the antagonist MK-801 alters GABAR function and subunit protein expression in a brain region-dependent manner, i.e. in the hippocampus, but not cerebral cortex. Regulation of excitatory synaptic receptors following impairment or enhancement of synaptic inhibition has not been as intensively examined, though regulation of excitatory receptors was recently demonstrated following chronic BZ exposure. Significantly increased levels of GluR1 subunit mRNA and protein were detected in the hippocampal CA1 region and frontal cortex of rats following a more intense 14-day diazepam treatment (Izzo et al., 2001). Increased GluR1 subunit protein was detected in pyramidal cell bodies and dendritic fields of the CA1 region using a sensitive immunogold detection technique. These increases were detected 96 h after discontinuation of diazepam treatment and correlated with the appearance of withdrawal signs indicating BZ dependence (Izzo et al., 2001). Absence of significant changes in CA1 region AMPAR subunit proteins in the present study may be attributable to the less sensitive immunohistochemical methods employed. Moreover, given the less intense 1-week FZP treatment and lack of overt behavioral dependence at 48 hours following treatment, lack of regulation in AMPAR subunit proteins may not be surprising. However, the increased mEPSC amplitude in CA1 neurons 48 h after treatment may indicate a physiological mechanism that in time, or if greater in magnitude, may contribute to behavioral manifestations of dependence. These findings together with enhanced AMPAR-mediated function present in this study suggest that changes in levels of excitatory neurotransmission following chronic BZ exposure may represent dynamic changes in the homeostatic balance of neuronal excitation/inhibition. Dynamic maintenance of neuronal excitatory/inhibitory homeostasis occurs over a period of days *in vitro* and is at least partially mediated by changes in the numbers of postsynaptic glutamate receptors

(O'Brien et al., 1998; Turrigiano and Nelson, 2000). Therefore, it will be important to establish the relative time-course of changes in inhibitory and excitatory receptor structure/function following chronic FZP treatment. Taken together, the data suggest that, *in vivo*, a reciprocal interaction exists between hippocampal GABAergic and glutamatergic transmitter systems, notably in the CA1 region.

4.5. Conclusion

The current study establishes increased AMPAR-mediated mEPSC amplitude and localized increases in AMPAR number in CA1 pyramidal neurons following 1-week FZP treatment. This physiological and anatomical evidence suggests a possible role for excitatory amino acid receptors in expression of BZ anticonvulsant tolerance. Impaired GABAergic function together with enhanced excitatory activity supports a dual mechanism for reduced BZ anticonvulsant effectiveness in rats following chronic BZ administration. Moreover, as FZP-treated rats are tolerant, but not overtly dependent (Tietz and Rosenberg, 1988), the possibility that increased CA1 pyramidal neuron excitability, manifest by increased AMPAR-mEPSC amplitude, may represent an early withdrawal phenomenon and thus contribute to BZ dependence and abuse liability cannot be discounted (Jackson et al., 2000). Changes in excitatory amino acid receptor function may accompany or contribute to BZ anticonvulsant tolerance or emerging dependence, and thus, excitatory amino acid receptors may provide a novel therapeutic target for restoring BZ effectiveness or limiting BZ abuse.

Acknowledgements

We would like to thank Dr. Robert Wenthold for providing the GluR2-specific antibody used in this study and Eugene Orłowski for technical assistance. We would also like to thank Dr. L. John Greenfield, Jr and Scott Lilly for helpful comments regarding the final manuscript. This work was supported by National Institutes of Health Grant Nos R01-DA0475 (to E.I.T.), F30-DA0604 (to B.J.V.) and a predoctoral fellowship (to B.J.V.) from the Medical College of Ohio.

References

- Barnes, E.M. Jr., 1996. Use-dependent regulation of GABA_A receptors. *International Reviews in Neurobiology* 39, 53–76.
- Bayazitov, I., Kleschevnikov, A., 2000. Afferent high strength tetanizations favour potentiation of the NMDA vs. AMPA receptor-mediated component of field EPSP in CA1 hippocampal slices of rats. *Brain Research* 866, 188–196.

- Blackstad, T.W., 1963. Ultrastructural studies on the hippocampal region. *Progress in Brain Research* 3, 122–148.
- Blahos, J. II, Wenthold, R.J., 1996. Relationship between N-methyl-D-aspartate receptor NR1 splice variants and NR2 subunits. *Journal of Biological Chemistry* 271, 15669–15674.
- Buller, A.L., Larson, H.C., Schneider, B.E., Beaton, J.A., Morrisett, R.A., Monaghan, D.T., 1994. The molecular basis of NMDA receptor subtypes: native receptor diversity is predicted by subunit composition. *Journal of Neuroscience* 14, 5471–5484.
- Chen, S., Huang, X., Zeng, X.J., Sieghart, W., Tietz, E.I., 1999. Benzodiazepine-mediated regulation of $\alpha 1$, $\alpha 2$, $\beta 1$ –3 and $\gamma 2$ GABA_A receptor subunit proteins in the rat brain hippocampus and cortex. *Neuroscience* 93, 33–44.
- Clements, J.D., Lester, R.A.J., Tong, G., Jahr, C.E., Westbrook, G.L., 1992. The time course of glutamate in the synaptic cleft. *Science* 258, 1498–1501.
- Crépel, V., Khazipov, R., Ben-Ari, Y., 1997. Blocking GABA_A inhibition reveals AMPA- and NMDA-receptor-mediated polysynaptic responses in the CA1 region of the rat hippocampus. *Journal of Neurophysiology* 77, 2071–2082.
- Derkach, V., Barria, A., Soderling, T.R., 1999. Ca²⁺/calmodulin-kinase II enhances channel conductance of alpha-3-hydroxy-5-methyl-4-isoxazolepropionate type glutamate receptors. *Proceedings of the National Academy of Science* 96, 3269–3274.
- Dingledine, R., Borges, K., Bowie, D., Traynelis, S.F., 1999. The glutamate receptor ion channels. *Pharmacological Reviews* 51, 7–61.
- Escalapez, M., Hirsch, J.C., Ben-Ari, Y., Bernard, C., 1999. Newly formed excitatory pathways provide a substrate for hyperexcitability in experimental temporal lobe epilepsy. *The Journal of Comparative Neurology* 408, 449–460.
- Gault, L.M., Siegel, R.E., 1998. NMDA receptor stimulation selectively initiates GABA_A receptor δ subunit mRNA expression in cultured rat cerebellar granule neurons. *Journal of Neurochemistry* 70, 1907–1915.
- Hirsch, J.C., Agassandian, C., Merchán-Pérez, A., Ben-Ari, Y., DeFilipe, J., Escalapez, M., Bernard, C., 1999. Deficit of quantal release of GABA in experimental temporal lobe epilepsy. *Nature Neuroscience* 2, 499–500.
- Houser, C.R., Escalapez, M., 1996. Vulnerability and plasticity of the GABA system in the pilocarpine model of spontaneous recurrent seizures. *Epilepsy Research* 26, 207–218.
- Huang, X., Chen, S., Tietz, E.I., 1996. Immunocytochemical detection of regional protein changes in rat brain sections using computer-assisted image analysis. *Journal of Histochemistry and Cytochemistry* 44, 981–987.
- Izzo, E., Auta, J., Impagnatiello, F., Pesold, C., Guidotti, A., Costa, E., 2001. Glutamic acid decarboxylase and glutamate receptor changes during tolerance and dependence to benzodiazepines. *Proceedings of the National Academy of Science* 98, 3483–3488.
- Jackson, A., Mead, A.N., Stephens, D.N., 2000. Behavioural effects of α -amino-3-hydroxy-5-methyl-4-isoxazolepropionate-receptor antagonists and their relevance to substance abuse. *Pharmacology & Therapeutics* 88, 59–76.
- Karczkubicha, M., Liljequist, S., 1995. Effects of post-ethanol administration of NMDA and non-NMDA receptor antagonists on the development of ethanol tolerance in C57BI mice. *Psychopharmacology* 120, 49–56.
- Kest, B., McLemore, G., Kao, B., Inturrisi, C.E., 1997. The competitive alpha-amino-3-hydroxy-5-methylisoxazole-4-propionate receptor antagonist LY293558 attenuates and reverses analgesic tolerance to morphine but not to delta or kappa opioids. *Journal of Pharmacology and Experimental Therapeutics* 283, 1249–1255.
- Macdonald, R.L., Olsen, R.W., 1994. GABA_A receptor channels. *Annual Review of Neuroscience* 17, 569–602.
- Mathews, D.B., Kralic, J.E., Devaud, L.L., Fritschy, J.M., Morrow, A.L., 2000. Chronic blockade of N-methyl-D-aspartate receptors alters γ -aminobutyric acid type A receptor peptide expression and function in the rat. *Journal of Neurochemistry* 74, 1522–1528.
- Mutel, V., Trube, G., Klingelschmidt, A., Messer, J., Bleuel, Z., Hummel, U., Clifford, M.M., Ellis, G.J., Richards, J.G., 1998. Binding characteristics of a potent AMPA receptor antagonist [³H]Ro48 8587 in rat brain. *Journal of Neurochemistry* 71, 418–426.
- Nusser, Z., Lujan, R., Laube, G., Roberts, J.D.B., Molnar, E., Somogyi, P., 1998. Cell type and pathway dependence of synaptic AMPA receptor number and variability in the hippocampus. *Neuron* 21, 545–559.
- O'Brien, R.J., Kamboj, S., Ehlers, M.D., Rosen, K.R., Fischbach, G.D., Huganir, R.L., 1998. Activity-dependent modulation of synaptic AMPA receptor accumulation. *Neuron* 21 (1067–107).
- Papp, E., Leinekugel, X., Henze, D.A., Lee, J., Buzsáki, G., 2001. The apical shaft of CA1 pyramidal cells is under GABAergic interneuronal control. *Neuroscience* 102, 715–721.
- Petralia, R.S., Wenthold, R.J., 1992. Light and electron immunocytochemical localization of AMPA-selective glutamate receptors in the rat brain. *Journal of Comparative Neurology* 318, 329–354.
- Petralia, R.S., Wang, Y.-X., Mayat, E., Wenthold, R.J., 1997. Glutamate receptor subunit 2-selective antibody shows a differential distribution of calcium-impermeable AMPA receptors among populations of neurons. *Journal of Comparative Neurology* 385, 456–476.
- Poisbeau, P., Williams, S., Mody, I., 1997. Silent GABA_A synapses during flurazepam withdrawal are region specific in the hippocampal formation. *Journal of Neuroscience* 17, 3467–3475.
- Rosenberg, H.C., 1995. Differential expression of benzodiazepine anticonvulsant cross-tolerance according to time following flurazepam or diazepam treatment. *Pharmacology, Biochemistry and Behavior* 51, 363–368.
- Shi, S.H., Hayashi, Y., Petralia, R.S., Zaman, S.H., Wenthold, R.J., Svoboda, K., Malinow, R., 1999. Rapid spine delivery and redistribution of AMPA receptors after synaptic NMDA receptor activation. *Science* 284, 1811–1816.
- Staley, K.J., Soldo, B.L., Proctor, W.R., 1995. Ionic mechanisms of neuronal excitation by inhibitory GABA_A receptors. *Science* 269, 977–981.
- Steppuhn, K.G., Turski, L., 1993. Diazepam dependence prevented by glutamate antagonists. *Proceedings of the National Academy of Science* 90, 6889–6893.
- Tietz, E.I., Rosenberg, H.C., 1988. Behavioral measurement of benzodiazepine tolerance and GABAergic subsensitivity in the substantia nigra pars reticulata. *Brain Research* 438, 41–51.
- Tietz, E.I., Huang, X., Chen, S., Ferencak, W.J. III, 1999. Temporal and regional regulation of $\alpha 1$, $\beta 2$ and $\beta 3$, but not $\alpha 2$, $\alpha 4$, $\alpha 5$, $\alpha 6$, $\beta 1$ or $\beta 2$ GABA_A receptor subunit mRNAs following one week oral flurazepam administration. *Neuroscience* 91, 327–341.
- Turrigiano, G.G., Nelson, S.B., 2000. Hebb and homeostasis in neuronal plasticity. *Current Opinions in Neurobiology* 10, 358–364.
- Wang, X.-H., Zhu, W.J., Corsi, L., Ikonovic, S., Paljug, W.R., Vicini, S., Grayson, D.R., 1998. Chronic dizocilpine (MK-801) reversibly delays GABA_A receptor maturation in cerebellar granule neurons *in vitro*. *Journal of Neurochemistry* 71, 693–704.
- Wenthold, R.J., Petralia, R.S., Blahos, J. II, Niedzielski, A.S., 1996. Evidence for multiple AMPA receptor complexes in hippocampal CA1/CA2 neurons. *Journal of Neuroscience* 16, 1982–1989.
- Wyllie, D.J.A., Manabe, T., Nicoll, R.A., 1994. A rise in postsynaptic Ca²⁺ potentiates miniature excitatory postsynaptic currents and AMPA responses in hippocampal neurons. *Neuron* 12, 127–138.
- Xie, X.H., Tietz, E.I., 1992. Reduction in potency of selective γ -aminobutyric acid, agonists and diazepam in CA1 region of *in vitro* hippocampal slices from chronic flurazepam-treated rats.

- Journal of Pharmacology and Experimental Therapeutics 262, 204–211.
- Zeng, X., Tietz, E.I., 1999. Benzodiazepine tolerance at GABAergic synapses on hippocampal CA1 pyramidal cells. *Synapse* 31, 263–277.
- Zeng, X., Xie, X.H., Tietz, E.I., 1995. Reduction of GABA-mediated IPSPs in hippocampal CA1 pyramidal neurons following oral flurazepam administration. *Neuroscience* 66, 87–99.
- Zhu, W.J., Vicini, S., Harris, B.T., Grayson, D.R., 1995. NMDA-mediated modulation of γ -aminobutyric acid type A receptor function in cerebellar granule neurons. *Journal of Neuroscience* 15, 7692–7701.